modes of electrical conductivity that are excited by the small amounts of energy released when an infrared photon is absorbed.

36. For wavelengths no longer than 200 μm, the detectors will work on a different principle. With proper doping, silicon and germanium can be made to have electrical resistance strongly dependent on temperature (not photon absorption rate). This material can be used to make detectors sensitive to any wavelength of light that they can absorb. To provide adequate sensitivity for SIRTF, such detectors will have to be cooled with an auxiliary refrigerator to 0.1 to 0.3 K.
37. The Rayleigh criterion states that point sources of equal brightness can only be distinguished if they are separated by an angle (in radians) of at least $1.2\,\lambda/D$, where λ is the wavelength of observation and D is the diameter of the telescope. Means to improve on this criterion are discussed, for example, by B. R. Frieden and J. J. Burke [*J. Opt. Soc. Am.* **62**, 1202 (1972)].
38. D. Downes, R. Genzel, E. E. Becklin, C. G. Wynn-Williams, *Astrophys. J.* **244**, 869 (1981).
39. D. M. Watson, in *Galactic and Extragalactic Infrared Spectroscopy*, M. F. Kessler and J. P. Phillips, Eds. (Reidel, Dordrecht, 1984), p. 195.
40. H. J. Habing *et al.*, *Astrophys. J.* **278**, L59 (1984).
41. P. W. Hodge, *Atlas of the Andromeda Galaxy* (Univ. of Washington Press, Seattle, 1981).
42. We thank K. Taylor, L. Yule, and a number of Riekes (particularly F. Rieke) for assistance in preparing this article.

Dynamics of Fractal Networks

R. ORBACH

Random structures often exhibit fractal geometry, defined in terms of the mass scaling exponent, D, the fractal dimension. The vibrational dynamics of fractal networks are expressed in terms of the exponent $\bar{\bar{d}}$, the fracton dimensionality. The eigenstates on a fractal network are spatially localized for $\bar{\bar{d}}$ less than or equal to 2. The implications of fractal geometry are discussed for thermal transport on fractal networks. The electron-fracton interaction is developed, with a brief outline given for the time dependence of the electronic relaxation on fractal networks. It is suggested that amorphous or glassy materials may exhibit fractal properties at short length scales or, equivalently, at high energies. The calculations of physical properties can be used to test the fractal character of the vibrational excitations in these materials.

THE CONCEPT OF FRACTAL STRUCTURE, DEVELOPED BY Benoit Mandelbrot (*1*), has potential utility because it is possible that structures that appear purely random can be described within a geometric mathematical framework. Fractal concepts may describe not only the static geometrical properties of such structures but also their dynamical properties and interactions with external measurement probes. The purpose of this article is to introduce the basic concepts behind the use of fractal geometry in performing these operations.

The fractal description of nature has developed so rapidly and so broadly in recent years, and fractal geometry has become such a powerful tool, that it would be impossible to attempt complete coverage of this subject. Therefore, only the more universal aspects of the structural properties of fractal networks will be analyzed in this article; more specific applications have been described (*2*).

The class of fractal structures treated in this article is limited to those that exhibit "self-similar" geometry. This means that the structure's geometrical properties are indistinguishable as a function of length scale (or resolution). Examining the fractal with ever more finely divided "rulers" would not result in any discernable difference in geometry. Conversely, the length scale of measurement could not be determined solely from observation of the fractal structure. This behavior usually breaks down at very short length scales, appropriate to the atomic or "building block" regime. In many physical systems (such as the percolating network, described later), the structure also ceases to be fractal at very long length scales, where it appears homogeneous or continuous. Mandelbrot (*1*) was the first to determine that many structures in nature exhibit self-similar geometry.

The most easily understood fractal concept is that of density. For fractal structures, this means that there is no constant relation between mass and volume as the length scale is changed. The amount of mass inside a sphere of radius r for a homogeneous (or Euclidean) structure scales as $M(r) = Ar^d$, where A is a numerical constant and d is the spatial or Euclidean dimension (d is 3 in our usual world). Analogously, the amount of mass inside a sphere of radius r for a fractal structure with self-similar geometry scales as $M(r) = Br^D$, where B varies according to the "lacunarity" (*1*) and D is the fractal dimension. In general, D is less than or equal to d because of the "open" character of fractal structures. That is, they tend to exhibit inhomogeneous arrangements of particles, with large amounts of open spaces (voids) and irregular atomic arrangements.

We are now in a position to calculate the density (ρ) of particles inside a sphere of radius r (that is, of volume $V(r) = Cr^d$, where C is a constant) for a fractal structure:

$$\rho(r) = M(r)/V(r) = Br^D/Cr^d \propto r^{D-d} \tag{1}$$

For self-similar structures, the fractal dimension D does not depend on r. This is an extraordinary result, for it implies an order in structures that to a casual observer appear to be completely disordered. It is even more remarkable because densities in seemingly unrelated phenomena in nature appear to behave in such a manner (*1*).

Because D is less than or equal to d, the density falls off with increasing length scale, implying that fractal objects of large size would be extraordinarily light. This must be tempered with the

---

R. Orbach is in the Department of Physics, University of California, Los Angeles 90024.

remark that at short length scales the atomic local geometries may not be fractal, while at very long length scales the geometry may appear to be homogeneous, implying an upper cutoff for r for those situations in which Eq. 1 may apply. Beyond this upper cutoff, $\rho(r)$ would simply be a constant.

An example where only the lower limit is appropriate can be found in aggregates of silica particles produced by flame hydrolysis of $SiCl_4$, known commercially as the products Cab-O-Sil and Alfasil (*3*) (here, the structure is Euclidean for short length scales and fractal for long length scales). From the results of electron microscopy studies, these materials are known to consist of ramified aggregates of very small, nearly spherical SiO_2 units ($R \sim 25$ Å) that stick together to form clusters measuring approximately 1000 Å across. Small angle neutron-scattering studies (*4*) on normal, compressed, and water-suspended powders, ranging in density from 0.009 to 0.45 g cm^{-3}, measure particle densities that obey Eq. 1 [the number density of SiO_2 units in a cluster diminishes with increasing size (r) of the volume sampled by the neutron-scattering study]. The fractal dimensionality D is found to be 2.52 ± 0.05 for all the samples studied. This is an explicit example where D is less than d ($d = 3$).

An example of a structure that has an upper limit for the length scale over which the structure is fractal is the much-studied percolating network (*5*) [here, the structure is fractal for short length scales (but greater than a fundamental grid dimension) and Euclidean for long length scales]. This model is thought to describe various physical structures, such as gels (*6*), polymers (*7*), and the transverse force constants of glassy materials (*8*). It forms the basis for studies of the flow of liquids through material aggregates [for example, oil and water through sandstone (*9*)]. There are two kinds of percolating networks: site and bond. To create a site-percolation network, each intersection of a d-dimensional grid is occupied at random with probability p. Sites are said to be connected if they are adjacent along a principal direction (that is, along a vertical or horizontal direction in $d = 2$ for a square grid, but not along the diagonals). A bond-percolation network is created by laying down the elementary components that make up the grid at random with probability p. The sites are then those points where the elementary components touch. The two kinds of percolation networks are not simply related, except for some special cases (*5*). We shall work with site percolation exclusively in this article.

Remarkably, a critical probability p_c exists such that, for $p \geq p_c$, a connected cluster will cross the grid continuously from one side to the other. This is referred to as an infinite cluster because, for an infinitely large grid, it will be of infinite extent. In contrast, the remainder of the occupied sites will form clusters of finite size. The probability of an occupied site being on the infinite network, $P(p)$, is given by the characteristic exponent β through the scaling formula

$$P(p) \propto (p - p_c)^{\beta} \qquad (2)$$

We identify the lower cutoff for the percolating network to be a length a that forms the horizontal and vertical lengths that make up the elementary grid. An upper cutoff length exists for the percolating network (*5*); this is referred to as ξ_p. This quantity is usually termed the percolation correlation length, or the pair connectedness length for percolation. For $r \geq \xi_p$, the percolating network appears homogeneous, and the density ρ is a constant. The percolating network exhibits self-similar geometry for $a \leq r \leq \xi_p$. The occupied site density on the inifinite cluster is given by Eq. 1 (the average occupied site density is simply p). We say, therefore, that the percolating network is fractal for length scales r between $a \leq r \leq \xi_p$ and Euclidean for $r \geq \xi_p$. The upper cutoff length ξ_p exhibits the scaling relation (*5*)

$$\xi_p \simeq a|p - p_c|^{-\nu_p} \qquad (3)$$

For a site percolation network in $d = 2$, ν_p is 4/3 [this is the so-called den Nijs conjecture (*10*), now thought to be exact], β_p is 5/36 [also thought to be exact (*11*)], and p_c is 0.5928 [for bond percolation in $d = 2$, p_c is 0.5 (*5*)]. The fractal dimension D is approximately 1.9 (*12*).

For the site percolation networks ($d = 2$) pictured in Figs. 1 through 4 (*13*), the largest cluster is always shown in white, the second largest in bright yellow, the third in dull yellow, and successively smaller clusters in shades varying from orange to red to light blue. The clusters are formed on a square grid, with 3000 elementary sites on a side. Figure 2 is formed by setting the probability that a given site is occupied at $p = 0.593$, just above the critical percolation concentration p_c. The region within the small square drawn on Fig. 2 is expanded to full size in Fig. 3. Figures 2 and 3 cannot be distinguished geometrically; both obey Eq. 1 for the occupied site density on the infinite cluster (shown in white). This is an explicit example of self-similarity. Expansion or contraction of regions of Fig. 2 will look the same (that is, the site density on the infinite cluster will obey Eq. 1) as long as their size falls between the length scale limits $a \leq r \leq \xi_p$. The upper length scale ξ_p can be extracted from Fig. 2 as the size of the "largest hole" in the infinite network, or the largest cluster (shown in bright yellow). At smaller concentrations ($p < p_c$), ξ_p is the size of the largest cluster (shown in white on Fig. 1). At larger concentrations ($p > p_c$ as in Fig. 4), the infinite network encompasses more and more of the occupied sites according to Eq. 2. The correlation length can be relevant to other fractal structures. In the subsequent discussion, we retain the subscript p only when referring explicitly to the percolating network. The notation will be appropriate also for the exponents ν_p and β_p.

The fractal dimension for $d = 2$ site percolation can be obtained from Figs. 1 through 4 by drawing circles of successively increasing radii (limited, of course, always to $r < \xi_p$) and then counting the number of occupied sites of a given color lying within each circle. That number, divided by the Euclidean area, πr^2, will scale according to Eq. 1, giving D directly. The reader should be warned that there will be large fluctuations in the value found for $\rho(r)$, depending on where one chooses the origin for the circles. The magnitude of these fluctuations is a measure of the lacunarity (*1*). Averaging over a great many origins for a given circle size will result in a unique value for D. We denote this "ensemble" average by $<\ldots>$.

There are other indices besides the fractal dimension that are useful for the description of the purely static geometrical properties of fractal networks. An example is the minimum distance l traveled along the fractal network, restricted to paths between connected sites, when traversing the fractal from one point to another (for example, the minimum path length between two points on the infinite cluster for a path confined to the infinite cluster). This is termed the chemical length. It is not the same as the length L measured between the same two points with a straight edge (referred to as the Pythagorean length). The two can be related to one another by $l = Ld_{\min}$ (*14*). In general, $d_{\min}$ is greater than or equal to 1 for fractal networks (the equality holding in the Euclidean limit, when $L \geq \xi_p$). For a percolating network in $d = 3$, $d_{\min}$ is 1.39.

Although the concept of fractal geometry is useful for the definition of static structural properties, it can also have utility when describing the dynamical properties of fractal networks. These could arise either directly, as vibrations of the atoms that make up a fractal structure, or in terms of the diffusion or flow of particles along paths constrained to fractal geometry.

The most famous example of dynamics of a fractal network originated with de Gennes (*15*), who posed the following problem. An ant is dropped onto an occupied site of the infinite cluster of a percolating network. The ant takes steps at a constant rate of elementary length a that are random in direction to adjacent (connected) sites on the infinite network. What is the (ensemble) average mean square distance that the ant travels in a time t?

This problem was solved only recently by Gefen and colleagues (*16*). The solution opened the way for a nearly complete description of the dynamics of fractal networks. They showed that the mean square distance that the ant moves in time t along the fractal network (for example, an infinite cluster) could be mapped onto the diffusion problem in Euclidean space. The price paid is the substitution of a (Euclidean) length-dependent diffusion constant [that is, $D \rightarrow D(r)$, where r is the Pythagorean length] for the conventional diffusion constant. They showed that

$$D(r) \propto r^{-\theta}, r \leqslant \xi_p \tag{4}$$

where the constant θ equals 0 in the Euclidean limit. Inserting Eq. 4 into the diffusion equation [$<r^2(t)> = D(r)t$] and solving for r, a scaling relation

$$<r^2(t)> \propto t^{2/(2+\theta)} \tag{5}$$

is found for a fractal network. Here, the length r is the Pythagorean distance, but diffusion has been confined to paths between connected adjacent sites on the percolating network. The value of θ has been calculated to be approximately 0.8 in $d = 2$ and 1.5 in $d = 3$ for percolating networks (*17, 18*). Diffusion is distinctly slowed down on a percolating network compared to diffusion in Euclidean space: $<r^2(t)> \propto t^{0.57}$ for $d = 3$ compared to $<r^2(t)> \propto t$, respectively.

The fracton dimension, $\bar{\bar{d}}$, first introduced by Alexander and Orbach (*19*) (they initially termed it the spectral dimension), can now be defined by rewriting Eq. 5 as

$$<r^2(t)> \propto t^{\bar{\bar{d}}/D} \tag{6}$$

where

$$\bar{\bar{d}} = 2D/(2 + \theta) \tag{7}$$

Further, diffusion on a fractal network with $\bar{\bar{d}} < 2$ is recurrent (that is, there is always a finite probability of return to the origin). This enabled Rammal and Toulouse (*20*) [and later de Gennes (*21*)] to obtain the number of distinct sites visited by the ant, $S(t)$, during its random wanderings on the fractal network in time t. De Gennes noted that the number of distinct sites contained within a sphere of radius r is proportional to r^D, so that, from Eq. 6,

$$S(t) \propto r^D \propto [(t^{\bar{\bar{d}}/D})^{1/2}]^D \equiv t^{\bar{\bar{d}}/2}, r \leqslant \xi_p \tag{8}$$

This result has been confirmed by many investigators by means of numerical simulations, and it is in fact a method for determining $\bar{\bar{d}}$ (*18, 22*). Mandelbrot (*1*) has observed that $\bar{\bar{d}}/2$ is the fractal codimension of the recurrences of the ant to a previously visited site. The number of distinct sites visited in time t is determined solely by $\bar{\bar{d}}$ (Eq. 8), whereas the mean square distance traveled in the same time t depends on the ratio $\bar{\bar{d}}/D$ (Eq. 6).

Earlier, Alexander and Orbach noted (*19*) that $\bar{\bar{d}}$ is approximately 4/3, to the numerical accuracy then available for percolating networks for all dimensions d greater than or equal to 2 (it is exactly 4/3 for $d \geqslant 6$, the dimensionality at which mean field theory is exact for percolation). They suggested that $\bar{\bar{d}} = 4/3$ may be an exact relation for all d greater than or equal to 2. This has become known as the "Alexander-Orbach conjecture." It remains rather controversial (*17*) [however, see (*18, 23*)]. It does, however, provide an excellent first approximation and may yet be found to be exact (*23*).

There is another reason for the importance of the Alexander-Orbach conjecture. Should it be exact, the exponent t, determining the dependence of the electrical conductivity σ of a random resistor network upon concentration

$$\sigma \propto (p - p_c)^t \tag{9}$$

can be related to the static geometrical exponents ν and β defined earlier in Eqs. 2 and 3. Alexander and Orbach (*19*) showed that setting $\bar{\bar{d}}$ equal to 4/3 for a percolating network results in

$$t_p = \tfrac{1}{2}[\nu_p(3d - 4) - \beta_p] \tag{10}$$

As noted before, ν_p is 4/3 and β_p is 5/36 in $d = 2$ for a percolating network, leading to $t_p = 91/72 (\simeq 1.264)$ in $d = 2$. Recent numerical simulations give values for t_p that are closer to 1.3, or a value for $\bar{\bar{d}}$ of about 1.3 (*17*). However, Rammal and colleagues (*18*) find $\bar{\bar{d}} = 4/3$ to within numerical accuracy. A recent series expansion calculation (*23*) finds $\bar{\bar{d}} = 1.334 \pm 0.007$.

The fracton dimensionality may be most useful for the description of the vibrational dynamics of fractal networks. An example is the percolating network with each occupied site replaced by an identical mass and each bond replaced by an identical spring. Montroll (*24*) showed three decades ago that, if one could solve the problem of diffusion on such a network [here, the ant problem posed by de Gennes (*15*)], then the vibration problem of the geometrically equivalent network was automatically solved [for a force between atoms of the "scalar" type (*25*)].

It has already been noted that the geometry changes from fractal at short length scales ($a \leqslant r \leqslant \xi$) to Euclidean at large length scales ($r \geqslant \xi$). Short length scales mean high-frequency vibrations. These were termed fractons by Alexander and Orbach (*19*). Long length scales mean low-frequency vibrations. These are conventionally termed phonons (*26*). Thus, fractons are distinguished from phonons according to whether their wavelengths are short or long compared to ξ, respectively. We can associate the length ξ with a characteristic (or "crossover") frequency ω_c according to the relationship

$$\omega_c \propto \xi^{-D/\bar{\bar{d}}} \tag{11}$$

Thus, fracton frequencies are greater than ω_c, and phonon frequencies are less than ω_c.

The vibrational energy density of states $N(\omega)$ associated with a vibrating fractal network can be obtained easily. This quantity is important, for example, for the specific heat and the thermal conductivity of a fractal network. It is known (*26*) that $N(\omega)$ is proportional to $\omega^{\bar{\bar{d}}-1}$ for Euclidean structures in the Debye ($\omega < \omega_c$) regime. Alexander and Orbach (*19*) showed that $N(\omega)$ is proportional to $\omega^{\bar{\bar{d}}-1}$ in the fractal ($\omega > \omega_c$) regime. The form of $N(\omega)$ as a function of ω therefore depends on the excitation frequency of the fractal network. Thus, $N(\omega)$ is proportional to ω^2 for a $d = 3$ Euclidean structure in the Debye limit, whereas $N(\omega)$ is proportional to $\omega^{1/3}$ (from the Alexander-Orbach conjecture) for any $d \geqslant 2$ percolating network. This difference of behavior has been verified numerically (*27*) for percolating networks in $d = 2$ and $d = 3$. The precise shape of $N(\omega)$ in the vicinity of ω_c remains to be determined. A recent scaling analysis (*28*) suggests a bumplike structure in the vicinity of ω_c (Fig. 5).

Amorphous solids may exhibit fractal geometry at short length scales (*29*). Their vibrational density of states should follow the general outlines of Fig. 5. Recent inelastic neutron diffraction experiments (*30*) on vitreous silica (Fig. 6) exhibit $N(\omega)$ down to remarkably low vibrational energies: $\hbar\omega/k_B = 1.6$ K(k_B is Boltzmann's constant). The comparison with Fig. 5 is striking, but it should be stated that the shape of $N(\omega)$ has been attributed to a specific collective rotation of SiO_2 tetrahedra (perhaps the physical description of a vibrational excitation on a fractal network) (*30*).

In addition to describing the energy of vibrational excitations,

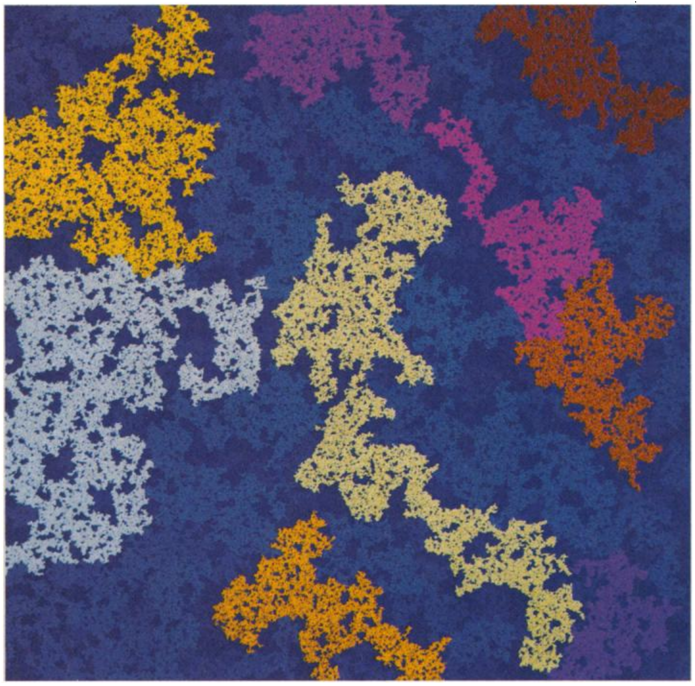

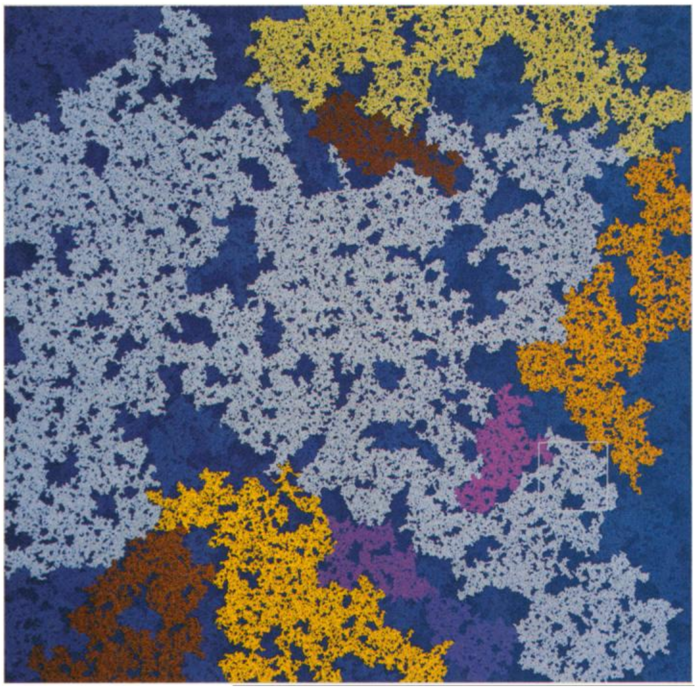

Fig. 1 (left). A percolation network, for sites at concentration $p = 59.00$ percent, occupied at random on a square grid of 3000 sites on a side, derived from periodic boundary conditions. Sites are considered connected if they are adjacent along a vertical or horizontal direction, not along the diagonals. The arrays of connected sites are clusters. The critical concentration for the largest cluster to span the grid from one side to another is 59.28 percent, in $d = 2$, so that this network is below the critical concentration. The size of the largest cluster (shown in white) is a measure of the percolation correlation length ξ_p at $p = 59.00$ percent. The structure is fractal for length scales $a \leq r \leq \xi_p$, where a is the fundamental grid size. [Reprinted with permission from R. F. Voss, IBM Thomas J. Watson Research Laboratories]

Fig. 2 (right). The same construction as in Fig. 1, but at $p = 59.30$ percent, just above the critical concentration for site percolation, $p_c = 59.28$ percent, in $d = 2$. The white cluster is now an infinite cluster (spanning the grid from one side to the other), and the percolation correlation length ξ_p is of the order of the next largest cluster (colored bright yellow). The structure is fractal for length scales $a \leq r \leq \xi_p$. [Reprinted with permission from R. F. Voss, IBM Thomas J. Watson Research Laboratories]

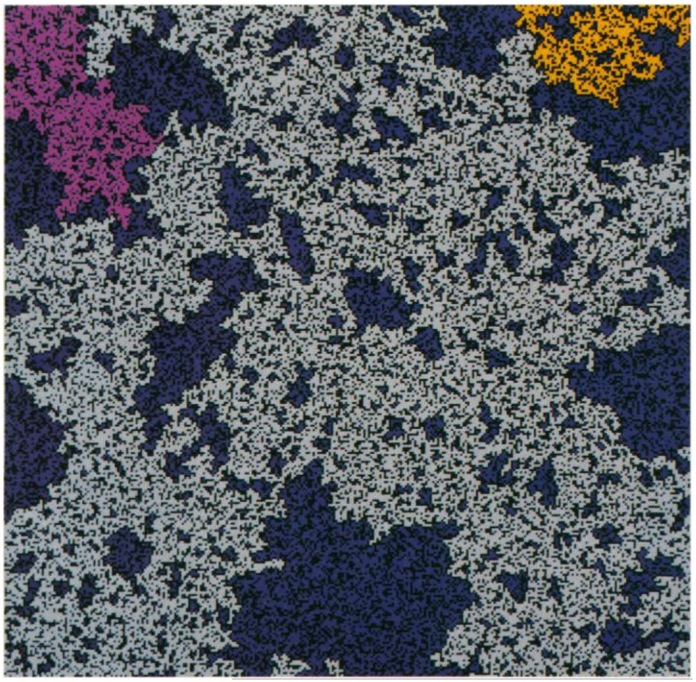

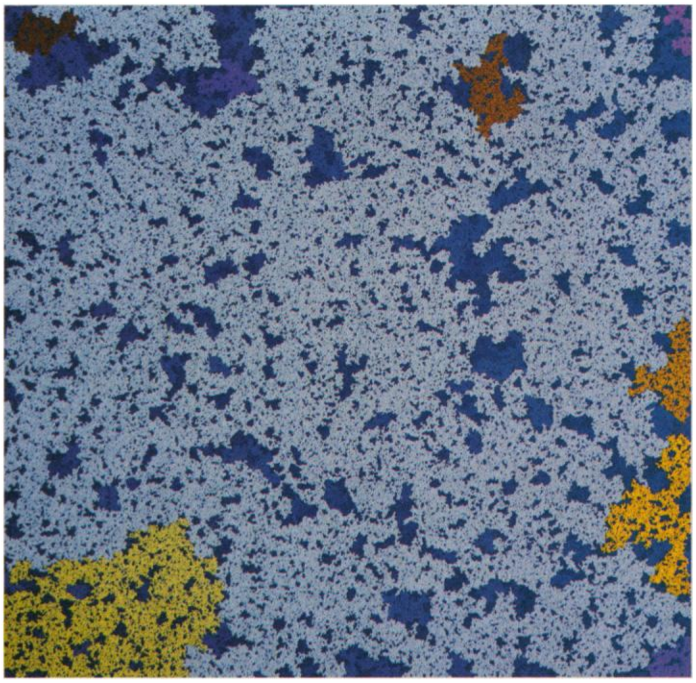

Fig. 3 (left). The expansion to full size of the small square in Fig. 2 (site percolation on a square grid at $p = 59.3$ percent). The grain is sufficiently large to observe the microscopic grid size. This is the lower limit a to fractal geometry. The average geometrical structure of the infinite cluster (shown in white) is the same as in Fig. 2. This is an illustration of self-similar geometry. [Reprinted with permission from R. F. Voss, IBM Thomas J. Watson Research Laboratories]

Fig. 4 (right). The same construction as in Fig. 1, but at $p = 59.60$ percent, above the critical concentration for site percolation, $p_c = 59.28$ percent, in $d = 2$. Again, ξ_p is the size of the largest hole (or the bright yellow cluster), and the structure is fractal for $r \leq \xi_p$. [Reprinted with permission from R. F. Voss, IBM Thomas J. Watson Research Laboratories]

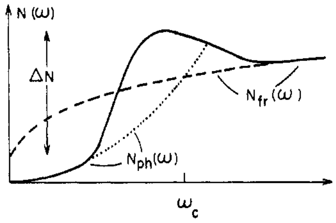

Fig. 5. A sketch of the density of vibrational states for a fractal network [the solid line, denoted $N_{fr}(\omega)$] plotted against frequency. The extrapolation of the low-frequency (long length scale) phonon density of states, $N_{ph}(\omega)$, is shown by a dotted line. The extrapolation of the high-frequency (short length scale) fracton density of states, $N_{fr}(\omega)$, is shown by the dashed line. [From (*28*)]

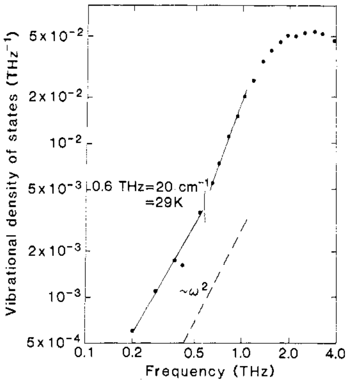

Fig. 6. A plot of the vibrational density of states for vitrous silica at 290 K. A line has been drawn at an energy that could reasonably be identified with the crossover from phonon to fracton excitations. Note the similarity to the predictions of Fig. 5. [Data replotted by U. Buchenau *et al.* (*30*)]

fractal geometry can also be useful for determination of the spatial extent of the vibrational wave function. This is particularly useful for random systems where explicit calculation of the wave function would be very difficult. There are two extremes: extended and localized. The former is the condition for homogeneous structures (weak disorder), where a plane wave is a useful first approximation. The latter is relevant to sufficiently strong disorder, where the wave function falls off exponentially (or more rapidly) with distance. Rammal and Toulouse (*20*) applied the scaling theory of localization (*31*) to excitations on a fractal network. The key parameter in that theory is the exponent β which governs the proportionality of the electrical conductance Σ for a random resistor network to the distance over which Σ is measured:

$$\Sigma(r) \propto r^{\beta} \tag{12}$$

For zero or negative β, the wave functions are localized. For positive β, they are extended. When applied to fractal networks, Rammal and Toulouse showed (*20*)

$$\beta = (D/\bar{\bar{d}})(\bar{\bar{d}} - 2) \tag{13}$$

For percolating networks, the Alexander-Orbach conjectures gives $\bar{\bar{d}} = 4/3$, leading to a strongly negative value for β. This results in localized fracton states.

The spatial extent of the localized fracton states, λ, depends on their excitation energy ω (*19*):

$$\lambda(\omega) \propto \omega^{-\bar{\bar{d}}/D} \tag{14}$$

This "dispersion law" depends only on the fracton and fractal dimensions. It is an example of how fractal geometry can simplify complex relations.

The form of the localized fracton wave function has been hypothesized (*32*) to be of the form

$$\phi(\omega) \propto (1/r^{d-D})\ [\lambda(\omega)]^{-D/2} \exp\{-\tfrac{1}{2}[r/\lambda(\omega)]^{d_\phi}\} \tag{15}$$

This is known (*33*) as "super-localization" because the exponent d_ϕ is bounded by unity and $d_{\min}$ and so in general is greater than unity. However, little is known about the precise shape of the fracton wave function in random structures (even for the well-studied percolating network), so that Eq. 15 should be regarded as a first approximation.

The localized character of fracton excitations can have profound implications. Consider, for example, the thermal conductivity of a fractal network. The long length scale (low-energy) vibrational excitations are phonons that, in $d = 3$, can be extended (because in Euclidean space $\bar{\bar{d}} = D = d$ and $\beta > 0$ in Eq. 13). The phonons are therefore able to carry heat from one spatial region to another. However, as the temperature increases, higher energy vibrations will be excited. Their energy is denoted by $\hbar\omega$, where thermal excitation means $\hbar\omega \sim k_BT$. When ω is approximately equal to ω_c, higher temperatures will excite fractons and not phonons (Fig. 5). However, fractons cannot carry heat from one spatial region to another because they are localized for $\bar{\bar{d}} < 2$. This means that k_BT will be much greater than the energy of those vibrational states that can carry heat (the phonons). Assuming a temperature-independent mean free path for the phonons then implies a thermal conductivity independent of temperature. Such a "plateau" in the thermal conductivity is common to nearly all amorphous solids (*34*). However, as the temperature is further increased, eventually the thermal conductivity is seen to increase. The origin of this increase has been attributed to thermal conductance arising from phonon-assisted fracton "hopping" (*35*) as a consequence of vibrational anharmonicity. The thermal conductivity is predicted (*35*) to increase linearly with increasing temperature, which is consistent with observation (*34*). Other interpretations (*36*) have also been offered for this behavior. They involve scattering processes off of "two-level systems" common to amorphous materials. The fracton-hopping picture is a "cleaner" explanation, but the matter is far from settled.

There are further implications of fracton localization. Excited states of localized electronic centers can relax nonradiatively by emitting one or more lattice vibrations (such processes are central to laser operation). Localized paramagnetic centers or nuclei relax toward thermal equilibrium (the so-called T_1 spin-lattice relaxation process) by inelastic scattering of lattice vibrations. These processes involve the interaction of electrons and lattice vibrations. Although the theory is well developed for phonons, an equivalent development has only recently been accomplished for fractons (*37*).

The simplest example is the one-vibrational quanta direct relaxation process (*38*). A localized electronic center relaxes to a lower energy state by emitting a lattice vibration, the energy of which is equal to the change in electronic energy. However, if the vibrational state is also localized, the two may lie farther away from one another than the localization length of the vibrational state (given for fractons by Eq. 14). The strength of the electron-fracton coupling for this particular pair of electron and fracton states would then be very small, inhibiting the electronic relaxation process. In general, there will be a distribution of distances between the electronic sites and the fractons that conserves energy in the relaxation process. This will result in an electronic relaxation rate that will vary from site to site. The probability density for the relaxation rate can be evaluated explicitly (*37*). The probability $P(t)$ to find the electron in its initial state after time t will vary at long times as

$$P_{\mathrm{direct}}(t) \propto t^{-(\ln t)^x} \tag{16}$$

where $x = (D/d_\phi) - 1$. For localized phonons, $D = d$ and $d_\phi = 1$, so that $x = 2$ in $d = 3$.

The direct-process electronic time relaxation profile (Eq. 16) is slower than exponential but faster than any power law. It is a direct consequence of localized vibrational states interacting with localized electronic sites. Extended vibrational states (phonons) will give rise to a single relaxation rate and an exponential time dependence for $P_{\mathrm{direct}}(t)$ in place of Eq. 16 (*38*).

Electronic (or nuclear) spin-lattice relaxation transitions involve relatively small changes in energy. The density of vibrational states at these small energies is too small to make the direct relaxation process effective. Rather, two vibrational states are involved, with the change in electronic (or nuclear) energy equaling the difference in the vibrational state energies. This is known as the Raman relaxation process (*38*). Extended vibrational states would again generate an exponential time dependence for $P(t)$. The temperature dependence varies as T^9 or T^7, depending on whether the electronic transition takes place between time-reversed states of half-integral spin (termed Kramers transitions) or not (termed non-Kramers transitions). Localized vibrational states again profoundly affect the time dependence of the Raman relaxation process. In the "near" long-time regime, the probability $P(t)$ to find the electron in its initial state after time t will vary as

$$P_{\text{Raman}}(t) \propto \exp[-t^{1/(a-2)}] \tag{17}$$

where $a = 4\bar{\bar{d}}(d_\phi/D) + 2\bar{\bar{d}}$ or $4\bar{\bar{d}}(d_\phi/D) + 2\bar{\bar{d}} - 2$ for Kramers or non-Kramers transitions, respectively. In the "far" long-time regime,

$$P_{\text{Raman}}(t) \propto t^{-(ln\ t)^{2D/d_\phi}} \tag{18}$$

which is similar to the time dependence of the direct process.

The calculation of the temperature dependence of the Raman relaxation process is greatly complicated by the nonexponential time dependence of both Eqs. 17 and 18. However, a simplification results when the (dipole-dipole or exchange) coupling between spins is sufficiently strong that the spins relax as a unit (that is, strong cross-relaxation). The time profile $P(t)$ is then exponential and is given by an average relaxation rate (written as an inverse relaxation time $1/T_1$), proportional to

$$(1/T_1)_{\text{Raman}} \propto T^{2\bar{\bar{d}}[1 + 2(d_\phi/D)] - 1} \qquad \text{(Kramers)} \tag{19a}$$

and

$$(1/T_1)_{\text{Raman}} \propto T^{2\bar{\bar{d}}[1 + 2(d_\phi/D)] - 3} \qquad \text{(non-Kramers)} \tag{19b}$$

These temperature dependences become $T^{2.63}$ and $T^{4.63}$, respectively, for a percolating network upon setting d_ϕ equal to d_{min}. Extended vibrational states would generate temperature dependences of T^9 and T^7, respectively. Experimental evidence for an anomalous temperature dependence for the Raman relaxation process has been obtained (*39*) for low-spin iron in large biological molecules.

These calculations demonstrate that local probes embedded in fractal networks should exhibit substantially different relaxation time profiles and temperature dependences as compared to Euclidean embeddings. Use of localized electronic probes in amorphous materials may be a direct test of the hypothesis that fractal geometry is a useful geometrical description at short length scales. The consequences of a fractal geometry are manifest through Eqs. 16 through 19.

REFERENCES AND NOTES

1. B. B. Mandelbrot, *The Fractal Geometry of Nature* (Freeman, New York, 1983); *Ann. Israel Phys. Soc.* **5**, 59 (1983); *J. Stat. Phys.* **34**, 895 (1984).
2. *J. Stat. Phys.* **36**, nos. 5 and 6 (1984); F. Family and D. P. Landau, Eds., *Kinetics of Aggregation and Gelation* (Elsevier/North-Holland, Amsterdam, 1984); *Scaling Phenomena in Disordered Systems* (NATO Advanced Study Institute, Geilo, Norway, April 1985) (Plenum, New York, 1985); H. E. Stanley, Ed., *Growth and Form* (Nijhoff, Amsterdam, 1985); L. Pietronero, Ed., *Fractals in Physics* (Elsevier/North-Holland, Amsterdam, 1986).
3. Cab-O-Sil is a trademark of the Cabot Corporation; Alfasil can be found as Stock Number D89376 (Alfa Catalog, 1981).
4. S. K. Sinha, T. Freltoft, J. Kjems, in *Kinetics of Aggregation and Gelation*, F. Family and D. P. Landau, Eds. (Elsevier/North-Holland, Amsterdam, 1984), p. 87.
5. A. Aharony, *J. Stat. Phys.* **34**, 931 (1984); D. Stauffer, *Introduction to Percolation Theory* (Taylor and Francis, London, 1985).
6. D. Stauffer, A. Coniglio, M. Adam, *Adv. Poly. Sci.* **44**, 103 (1982).
7. P. G. de Gennes, *Scaling Concepts in Polymer Physics* (Cornell Univ. Press, Ithaca, NY, 1979).
8. M. F. Thorpe, *J. Non-Cryst. Solids* **57**, 3155 (1983); H. He and M. F. Thorpe, *Phys. Rev. Lett.* **54**, 2107 (1985).
9. P.-G. de Gennes, *J. Phys. (Paris) Colloq.* **41**, C3/17 (1980); B. I. Halperin, S. Feng, P. N. Sen, *Phys. Rev. Lett.* **54**, 2391 (1985).
10. M. P. M. den Nijs, *J. Phys. A* **12**, 1857 (1979).
11. B. Nienhuis, E. K. Riedel, M. Schick, *ibid.* **13**, L189 (1980).
12. R. F. Voss, R. B. Laibowitz, E. I. Allessandrini, *Phys. Rev. Lett.* **49**, 1441 (1982); A. Kapitulnik and G. Deutscher, *ibid.*, p. 144.
13. Courtesy of R. F. Voss.
14. K. M. Middlemiss, S. G. Whittington, D. S. Gaunt, *J. Phys. A* **13**, 1835 (1980); R. Pike and H. E. Stanley, *ibid.* **14**, L169 (1981); D. C. Hong and H. E. Stanley, *ibid.* **16**, L475 (1983); *ibid.*, p. L525; H. J. Herman, D. C. Hong, H. E. Stanley, *ibid.* **17**, L261 (1984); J. Vannimenus, J. P. Nodal, C. Martin, *ibid.*, p. L351; S. Havlin and R. Nossal, *ibid.*, p. L425; S. Havlin, Z. V. Djordjevic, I. Majid, H. E. Stanley, G. H. Weiss, *Phys. Rev. Lett.* **53**, 178 (1984).
15. P. G. de Gennes, *Recherche* **7**, 919 (1976).
16. Y. Gefen, A. Aharony, S. Alexander, *Phys. Rev. Lett.* **50**, 77 (1973).
17. D. C. Hong, S. Havlin, H. J. Hermann, H. E. Stanley, *Phys. Rev. B* **30**, 4083 (1984); J. G. Zabolitzky, *ibid.*, p. 4077; H. J. Herrmann, B. Derrida, J. Vannimenus, *ibid.*, p. 4080; C. J. Lobb and D. J. Frank, *ibid.*, p. 4090.
18. R. Rammal, J. C. Angles d'Auriac, A. Benoit, *ibid.*, p. 4087.
19. S. Alexander and R. Orbach, *J. Phys. (Paris) Lett.* **43**, L-625 (1982).
20. R. Rammal and G. Toulouse, *ibid.* **44**, L-13 (1983).
21. P.-G. de Gennes, *C. R. Acad. Sci. Ser. B* **296**, 881 (1983).
22. P. Argyrakis and R. Kopelman, *Phys. Rev. B* **29**, 511 (1984).
23. J. W. Essam and F. M. Bhatti, in preparation.
24. E. W. Montroll, in *Proceedings of the Third Berkeley Symposium on Mathematical Statistics and Probability* (Univ. of California Press, Berkeley, 1955), p. 209.
25. S. Alexander, *J. Phys. (Paris)* **45**, 1939 (1984).
26. C. Kittel, *Introduction to Solid State Physics* (Wiley, New York, ed. 5, 1976), p. 107.
27. I. Webman and G. Grest, *Phys. Rev. B* **31**, 1690 (1985); *J. Phys. (Paris) Lett.* **45**, L-1155 (1984).
28. A. Aharony, S. Alexander, O. Entin-Wohlman, R. Orbach, *Phys. Rev. B* **31**, 2565 (1985); see also the earlier work of P. F. Tua, S. J. Putterman, and R. Orbach [*Phys. Lett.* **98A**, 357 (1983)].
29. S. Alexander, C. Laermans, R. Orbach, H. M. Rosenberg, *Phys. Rev. B* **28**, 4615 (1983).
30. U. Buchenau, N. Nucker, A. J. Dianoux, *Phys. Rev. Lett.* **53**, 2316 (1984).
31. E. Abrahams, P. W. Anderson, D. C. Licciardello, T. V. Ramakrishnan, *ibid.* **42**, 673 (1979).
32. S. Alexander, O. Entin-Wohlman, R. Orbach, *Phys. Rev. B* **32**, 6447 (1985).
33. Y.-E. Levy and B. Souillard, unpublished results.
34. R. C. Zeller and R. O. Pohl, *Phys. Rev. B* **4**, 2029 (1971); M. P. Zeitlin and A. C. Anderson, *ibid.* **12**, 4475 (1975).
35. S. Alexander, O. Entin-Wohlman, R. Orbach, unpublished results.
36. V. G. Karpov and D. A. Parshin, *J. Exp. Theor. Phys. Lett.* **38**, 648 (1983).
37. S. Alexander, O. Entin-Wohlman, R. Orbach, *J. Phys. (Paris) Lett.* **46**, L-549 (1985); *ibid.*, p. L-555.
38. R. Orbach and H. Stapleton, in *Electronic Paramagnetic Resonance*, S. Geschwind, Ed. (Plenum, New York, 1972), p. 121.
39. H. J. Stapleton, J. P. Allen, C. P. Flynn, D. G. Stinson, S.Kurtz, *Phys. Rev. Lett.* **45**, 1456 (1980); J. P. Allen *et al.*, *Biophys. J.* **38**, 299 (1982).
40. I thank D. O. Raphael for critical reading of the manuscript. Supported by NSF grant DMR 84-12898.